**Cell Reports, Volume *25***

## Supplemental Information

# An Integrative Study of Protein-RNA Condensates Identifies Scaffolding RNAs and Reveals Players in Fragile X-Associated Tremor/Ataxia Syndrome

**Fernando Cid-Samper, Mariona Gelabert-Baldrich, Benjamin Lang, Nieves Lorenzo-Gotor, Riccardo Delli Ponti, Lies-Anne W.F.M. Severijnen, Benedetta Bolognesi, Ellen Gelpi, Renate K. Hukema, Teresa Botta-Orfila, and Gian Gaetano Tartaglia**

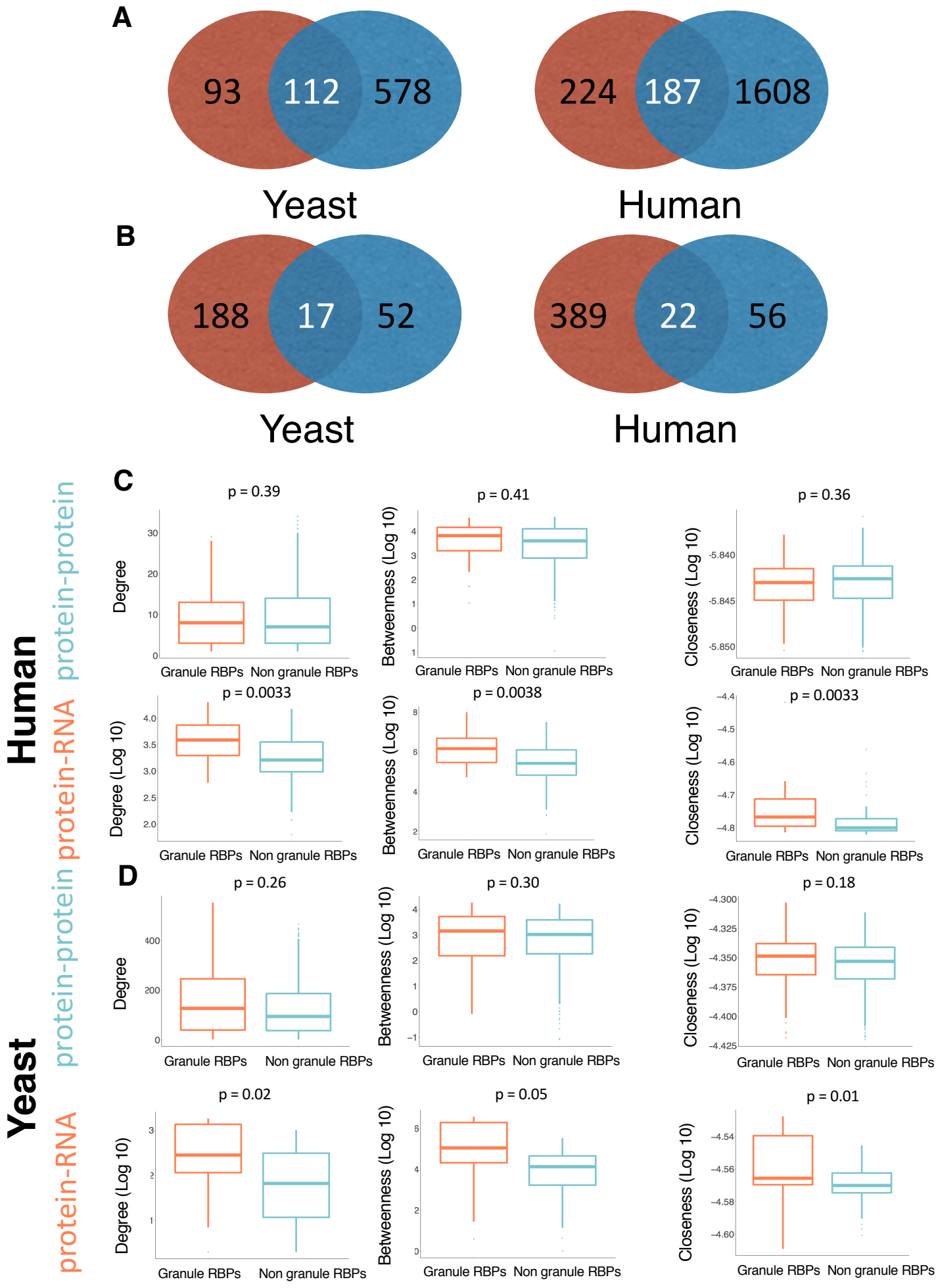


Supplementary Figure 1

**Supplementary Figure 1 [related to Figure 1]. Datasets A)** Granule RBPs Red circle: granule-forming proteins, Blue circle: RBPs, as defined in Gerstberger et al, 2014 (Gerstberger et al., 2014). Intersection represents granule RBPs. **B)** Number of interactions. Red circle: granule-forming proteins. Blue circle: RBPs with known targets. Intersection represents granule RBPs with known targets. **Distribution of centrality values of granule and non-granule RBPs in different interaction networks. C)** Centrality distributions for the human dataset. Up: Protein-protein network. (p-value (left) = 0.39, p-value (centre) = 0.41, p-value (right) = 0.36. Down: Protein-RNA network (p-value (left) = 0.003, p-value (centre) = 0.007, p-value (right) = 0.01. **D)** Centrality distributions for the yeast dataset. Up: Protein-protein network. (p-value (left) = 0.26, p-value (centre) = 0.30, p-value (right) = 0.18. Down: Protein-RNA network (p-value (left) = 0.02, p-value (centre) = 0.05, p-value (right) = 0.01.

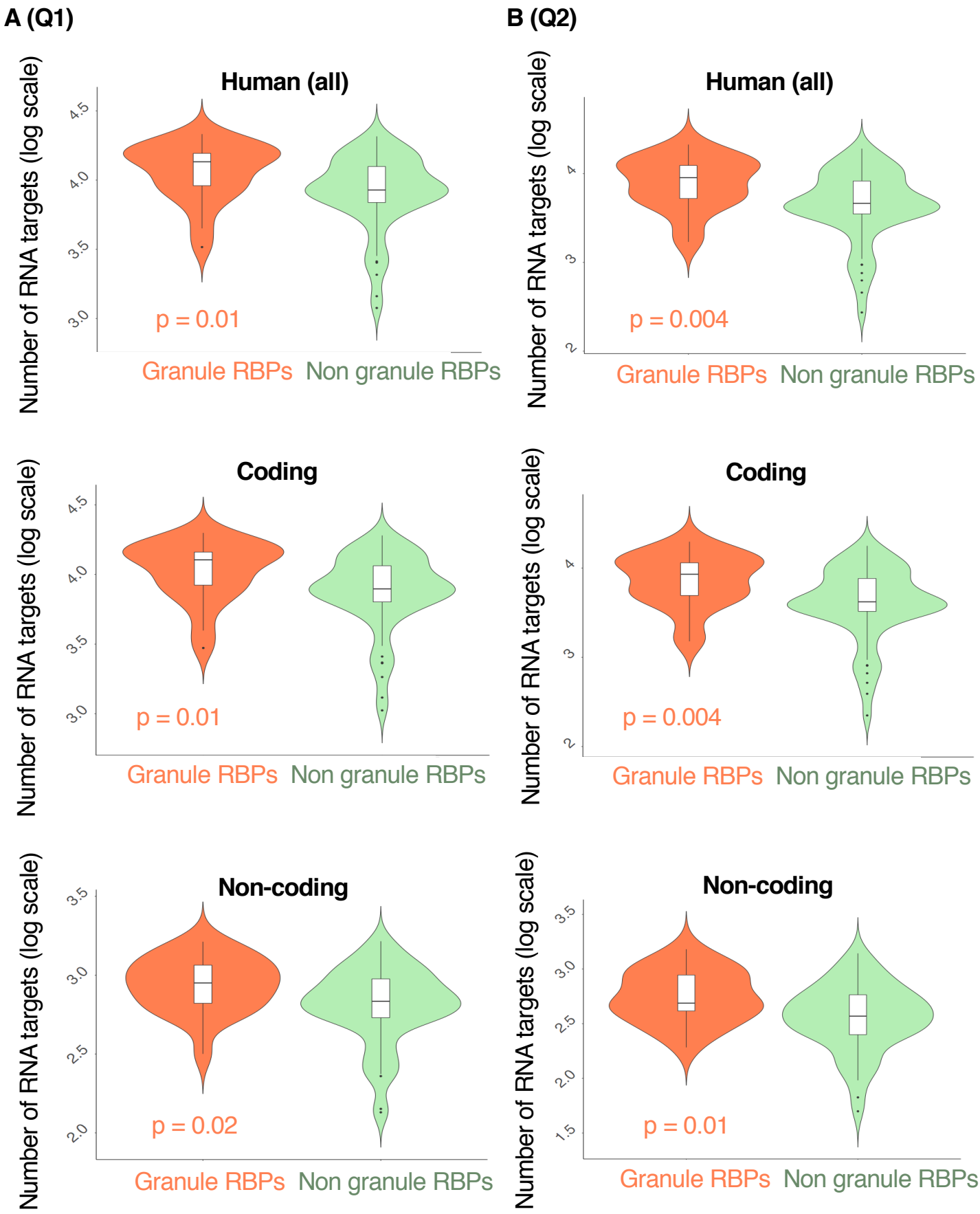


Supplementary Figure 2

**Supplementary Figure 2 [related to Figure 1]. Number of RNA targets of granule and non-granule RBPs: A)** First quartile of the reads/expression distribution (Q1). **B)** Second quartile (Q2).

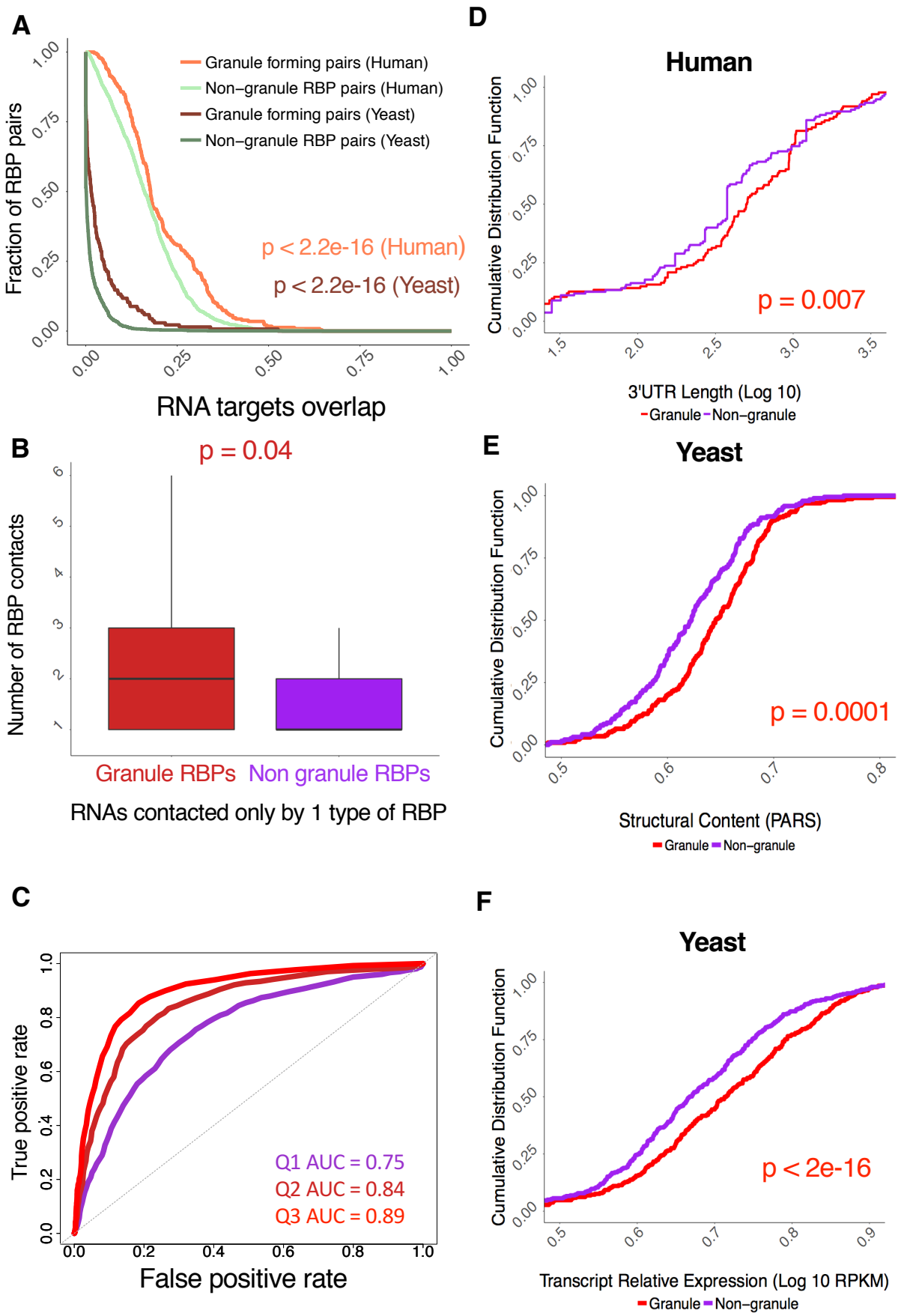


Supplementary Figure 3

**Supplementary Figure 3 [related to Figure 1,2]. Properties of granule RNAs. A)** RNAs interacting exclusively with granule forming RBPs have higher number of protein contacts (p-value = 0.04, Wilcoxon test). Human transcripts: **B)** Granule RNAs have more structured UTRs (p-value = 0.007; KS test). PARS analysis on 3'UTR of granule and non-granule RNAs**.** Yeast granule RNA are **C)** structured (p-value = 0.001; KS test; PARS data), and **D)** more abundant (p-value = 2.2e-16; KS test) than non-granule RNAs. The UTR analysis was not performed due to the lack of annotation.

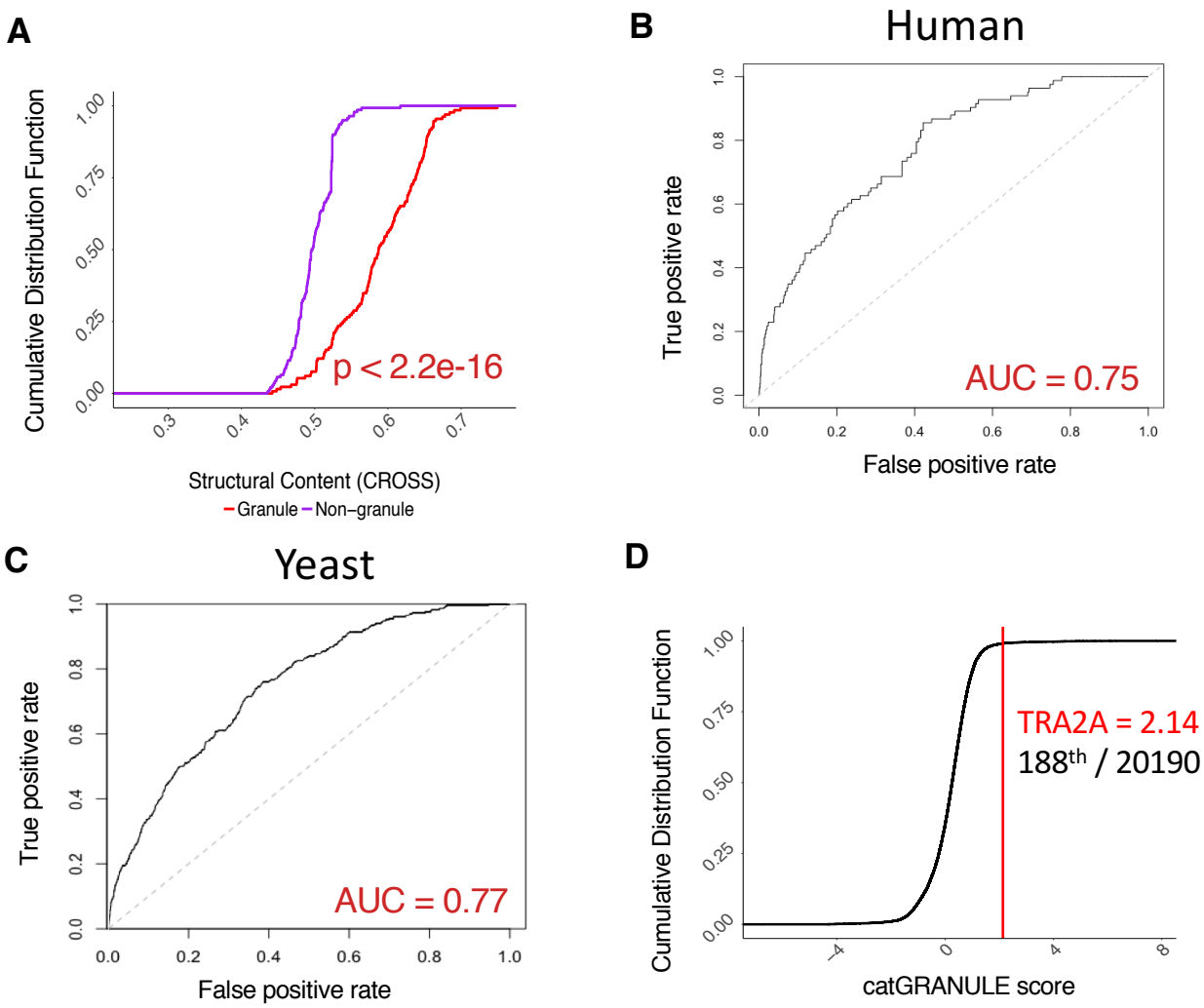


Supplementary Figure 4

**Supplementary Figure 4 [related to Figure 2,3]. Computational predictions of granule-forming components. A)** Granule transcripts are predicted to be more structured (structural content according is measured using CROSS; p-value < 2.2e-16, KS test). **B** and **C)** *cat*GRANULE performances on human and yeast experimentally described granule-forming proteins. AUC (Area under the ROC curve) is used to measure the discriminative power of the method. **D)** Distribution of *cat*GRANULE scores for the whole human proteome. TRA2A (*cat*GRANULE score = 2.14) ranks 188$^{th}$ out of 20190 human proteins (i.e. 1% of the distribution).

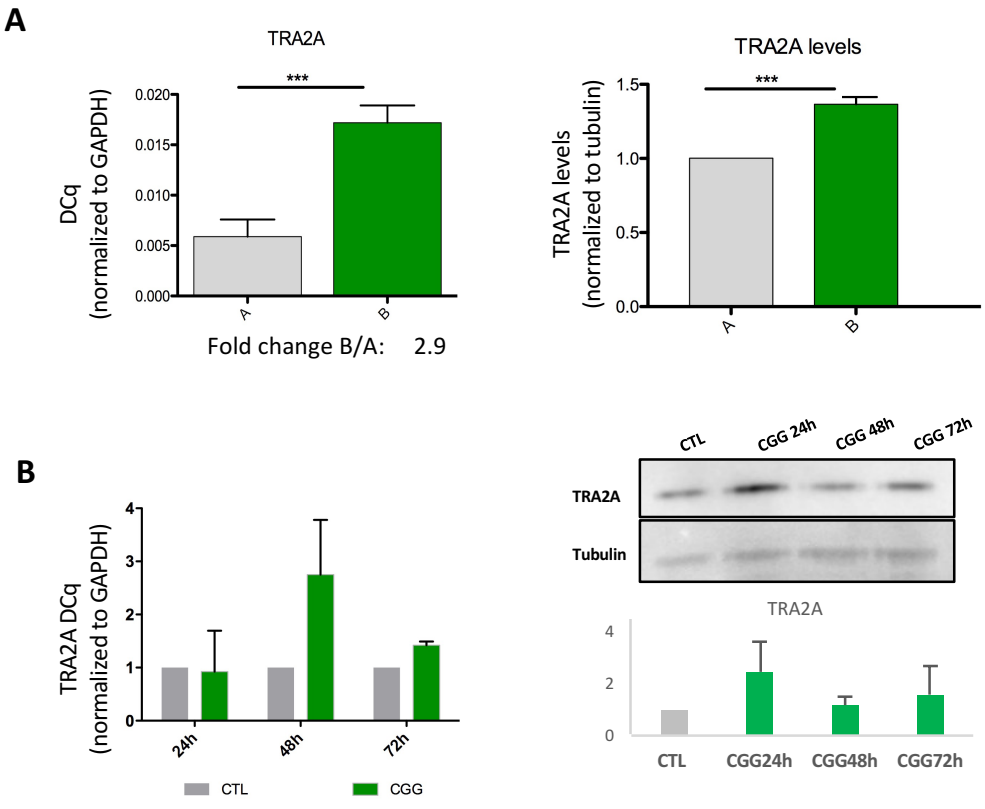


Supplementary Figure 5

**Supplementary Figure 5 [related to Figure 4]. TRA2A levels in human lymphocytes and COS-7 cell model. A)** Human lymphocytes from control (A) or pre mutation-carrier (B) were lysated and both RNA and protein were isolated (*** p-value < 0.01). Relative TRA2A RNA expression (left panel) and TRA2A protein (right panel) are represented. **B)** COS-7 cells were transfected with CGG(60X) and compared to controls. After 24h, 48h or 72h of transfection cells were pelleted and RNA and protein extraction was performed. Relative TRA2A RNA expression (left panel) and TRA2A protein (right panel) are represented.

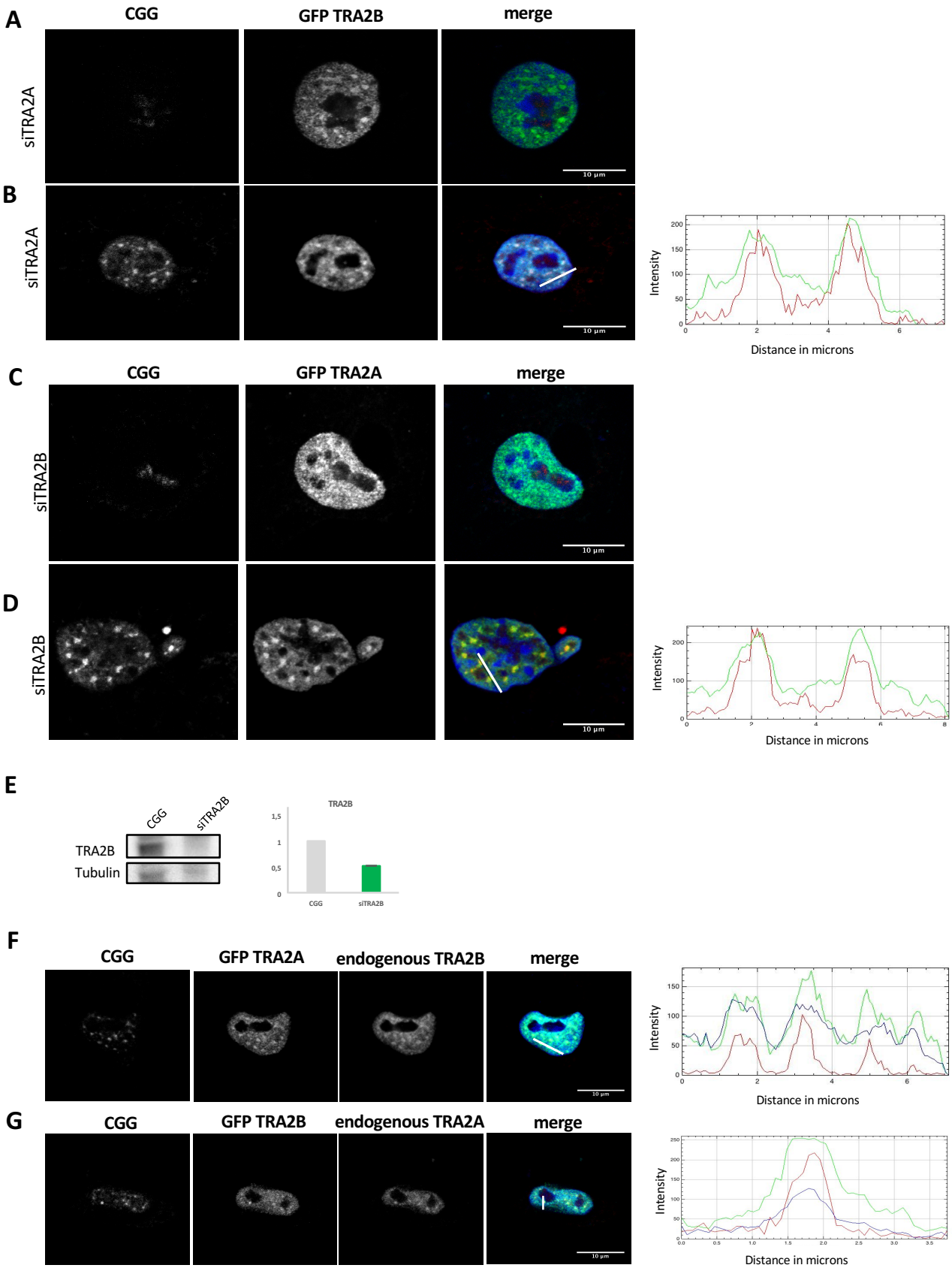


Supplementary Figure 6

**Supplementary Figure 6 [related to Figure 6]. TRA2B over-expression and TRA2A knock-down.** **A)** Control COS-7 cells (without CGG(60X) transfection) were transfected with GFP-TRA2B and siTRA2A. **B)** COS-7 cells were transfected with CGG(60X), GFP-TRA2B and siTRA2A. In both A and B, after 48 hours, cells were hybridized with Cy3-GGC(8X) probe and immunostained with an antibody against TRA2B. The graph represents TRA2B/CGG levels**. TRA2A over-expression and TRA2B knock-down. C)** Control COS-7 cells were transfected with siTRA2B and GFP-TRA2A (in absence of CGG(60X) transfection). **D)** COS-7 cells were transfected with CGG(60X), siTRA2B and GFP-TRA2A. In both A and B, after 48 hours of transfection cells were hybridized with Cy3-GGC(8X) probe and immunostained with antiGFP. The graphs represent TRA2A/CGG levels. **E)** TRA2B protein levels in COS-7 cells treated as in B. **TRA2A and TRA2B over-expression** COS-7 cells were transfected with GFP-TRA2A **F)** or GFP-TRA2B **G)** and CGG(60X). After 48 hours, cells were hybridized with Cy3-GGC(8X) probe and immunostained with an antibody against either TRA2A or TRA2B. Graphs represent TRA2A/TRA2B/CGG levels.

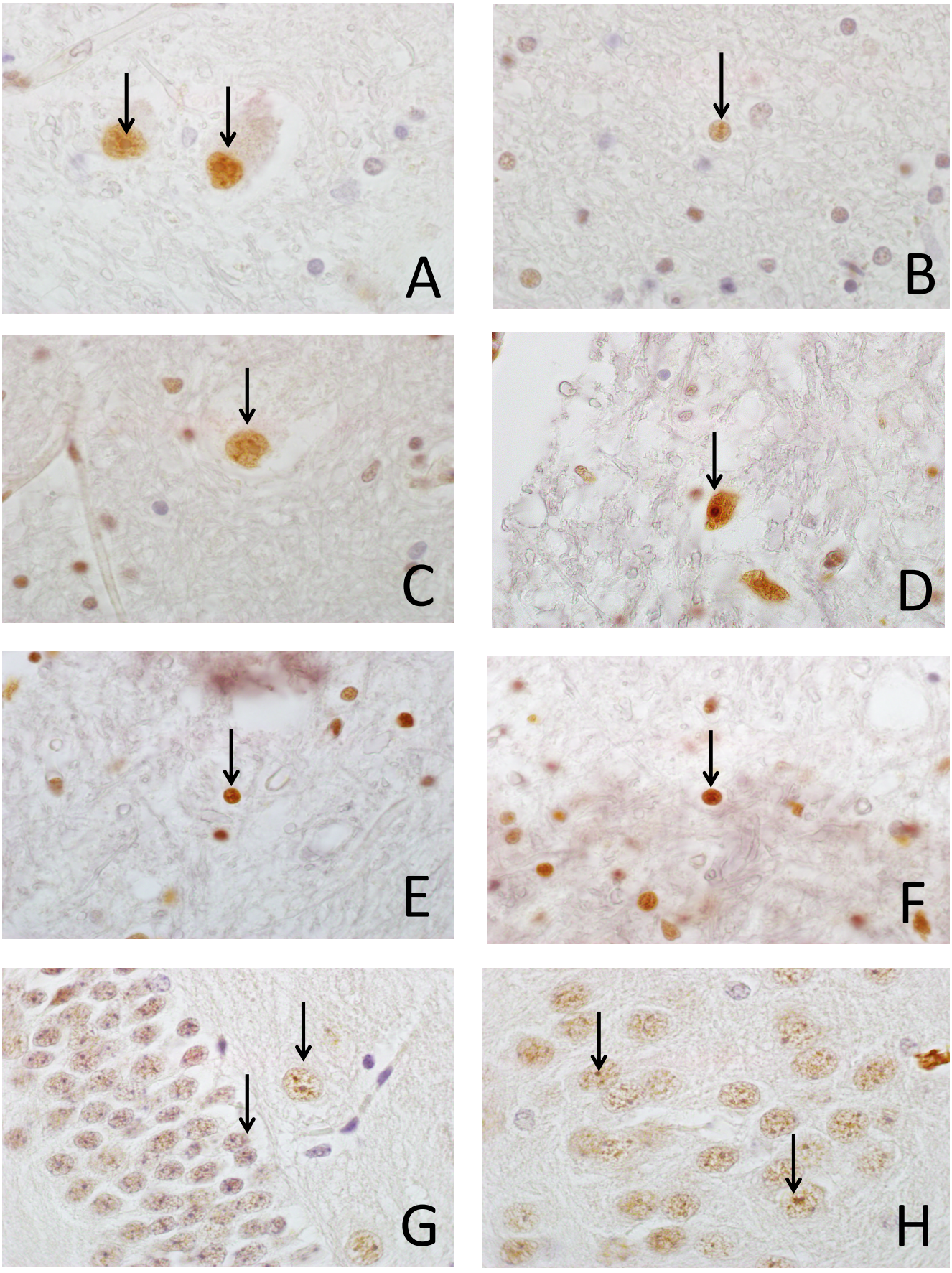


Supplementary Figure 7

**Supplementary Figure 7 [related to Figure 10]. A-F)** TRA2A immunohistochemistry in human hippocampus from FXTAS. **G-H)** TRA2A immunohistochemistry in premutated mouse model (counterstaining is done with haematoxylin; the arrows points to the inclusions).